Pulse Profile Rule in Laser Heating of Opaque Targets in Air

Bassam H. Habib*

Received 21, December, 2009
Accepted 11, July, 2010

Abstract:

A theoretical model is developed to determine time evolution of temperature at the surface of an opaque target placed in air for cases characterized by the formation of laser supported absorption waves (LSAW) plasmas. The model takes into account the power temporal variation throughout an incident laser pulse, (i.e. pulse shape, or simply: pulse profile).
Three proposed profiles are employed and results are compared with the square pulse approximation of a constant power.

Key words: Laser heating, Laser induced plasma, Laser plasma initiation.

Introduction:

When an opaque target is irradiated by laser energy of sufficient intensity, plasma may be generated. The status of this plasma depends strongly on experimental parameters such as laser radiation intensity, pulse duration and shape (profile) [1,2,3].
When the target is in an atmospheric environment and under certain experimental conditions, the laser-generated plasma forms what is known as Laser Supported Absorption Waves (LSAW) which is mainly due to the ionization of ambient air adjacent to target surface [4,5].
Once LSA-plasma is generated at target surface it begins to expand both axially (away from the surface, toward laser source) and laterally over target surface, in a manner similar (basically) to spherical blast wave expansion [5], this situation is illustrated schematically in fig.(1) [6].

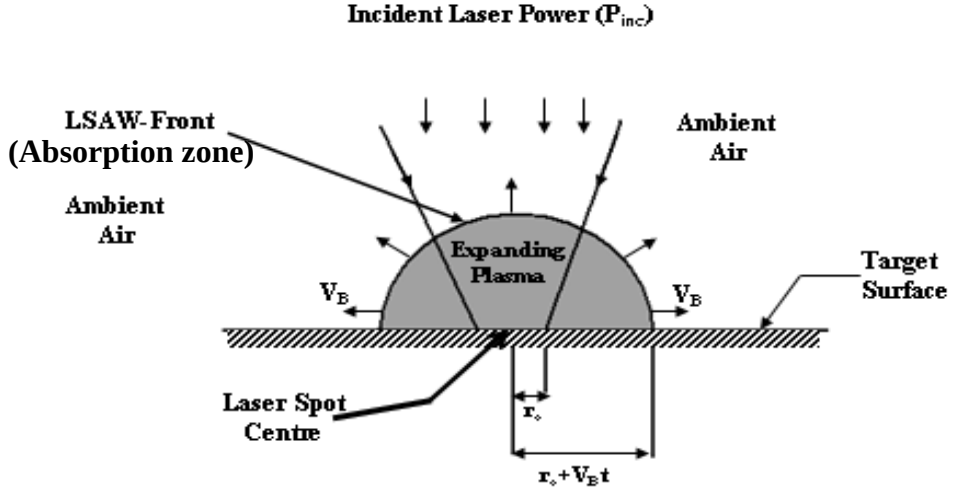

Fig.(1)

A scheme represents the expansion of LSA plasma over target surface in air.

*Al-Mansour University College,Computer Communication Engineering Department.

A fraction of incident laser energy is absorbed by LSAW- portion exposed to laser beam, known as absorption zone (see fig.1). The absorbed laser energy acts to sustain the LSA wave by heating the generated plasma [5].

The LSA plasma behaves in two contradictory ways in heating the target surface, on one hand; the laser generated plasma enhances the amount of heat energy transferred to the target (heat coupling), this heat coupling is due to both heat flow from plasma to the target through plasma-target interface via heat conduction, and u.v. radiation emitted by the plasma and absorbed by the target. On the other hand, the radial expansion of LSAW plasma causes the plasma-target contact area (interface) to increase (see fig.1) leading to a decrease in heat flux density on target surface due to energy spreading over surface area hence retarding the heating process [6].
Considering thermally thick targets, axial heat conduction from the surface through target bulk plays an additional rule in surface heating retardation.

The aim of this paper is to develop a computational model that tacks into account the laser pulse shape in simulating temperature evolution at the surface of an opaque, thermally thick target placed in air for situations where LSAW forms.

Surface Temperature

It was established that the change in temperature at the surface of an opaque target placed in air due to the action of an incident laser pulse is given as [6]:

$$\Delta T(\xi) = \frac{\mu_{eff} P_c k^{1/2}}{K(\pi\tau_p)^{3/2}} \int_0^{\xi} \frac{d\xi'}{(\xi')^{1/2}[r_o/\tau_p + V_B \times (\xi - \xi')]^2} \quad \ldots(1)$$

Equation (1) describes the situation shown in fig.(1) where LSAW-plasmas are formed. The parameters in this equation are as follows [6]:
μ_{eff} : Effective heat coupling coefficient, K, k: Thermal conductivity and diffusivity of target material respectively, V_B: Lateral blast velocity of expanding plasma (assigned a constant average value), r_o: Laser-spot radius, τ_p: Laser- pulse duration, ξ: A normalized time factor given as $\xi = t/\tau_p$ ($0 \le \xi \le 1$), Pc: Laser pulse power.
In eq.(1), the incident laser power was assumed constant throughout the pulse duration as depicted in fig.(2). It should be noted that eq.(1) takes into account the axial heat conduction from the surface to target bulk[6] .

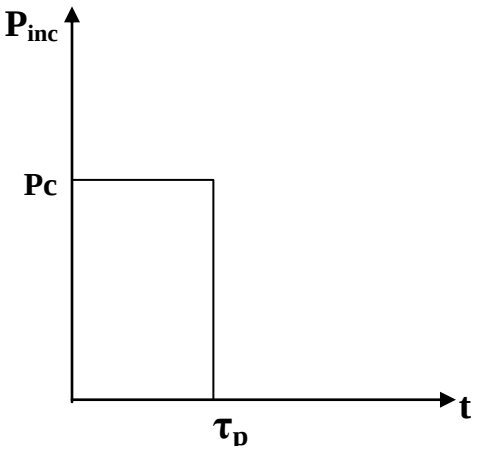

Fig(2):Representation of a rectangular laser pulse (square pulse).The incident power {P_{inc}} is constant (Pc) during the pulse duration (τ_p).

Under the assumptions of constant blast velocity (V_B) and pulse power (Pc), equation (1) may be integrated analytically to obtain surface temperature at any instant (ξ) during a single laser pulse [6]. Of course, the final temperature is obtained at ξ=1.

Present Modeling Features

In the present model, time dependence of incident power throughout a single

laser pulse is introduced in the determination of target surface temperature.

Time Dependence of Laser Power

It is more convenient to describe incident laser power [$P_{inc}(t)$] in terms of power density [I(t)] among laser spot area (A_o) since LSAW ignition condition is specified conventionally via power density factor [4,5] , hence we may write:

$$\mathbf{P_{inc}(t) = I(t) \cdot A_o \ldots (2)}$$

Here, time profile of I(t) [laser power density shape (or simply pulse shape)] is chosen such that average power density ($\bar{I}$) throughout the laser pulse lies within the range of LSAW-formation (~10^6 - 2 x 10^6 W/cm^2) [6] . Using time- variable power as represented by eq.(2) in the formulation of surface temperature yields an equation that corresponds to eq.(1), given as:

$$\Delta T(\xi) = B\int_0^{\xi} \frac{I(\xi-\xi')}{\xi'^{1/2}[\frac{r_o}{\tau_p}+V_B\times(\xi-\xi')]^2}d\xi' \quad \textbf{...(3)}$$

where $B = \dfrac{k^{1/2}\mu_{eff}\cdot A_o}{K(\tau_p\pi)^{3/2}}$, and $0 \le \xi \le 1$

for a single laser pulse duration.

In the present work, the time dependence of incident laser pulse is introduced via mathematical expressions chosen for the power density (I) in the integrand of eq.(3).

Equation (3) is then solved numerically to determine temporal surface temperature evolution throughout a single laser pulse.

Mathematical Expressions for Laser Pulses

To investigate the rule of laser pulse shape (profile) on target surface temperature, three mathematical forms are proposed for laser pulse shape (i.e. power density as a function of time), namely: exponentially decreasing, exponentially increasing, and Gaussian pulse.

As an approximation in this model, only that part of the profile exceeding LSA threshold (~ 10^6W/cm^2) is included in solving eq.(3) numerically, accordingly, the pulse duration (τ_p) is regarded as the duration of that part exclusively, as illustrated in fig.(3) for the three proposed pulses.

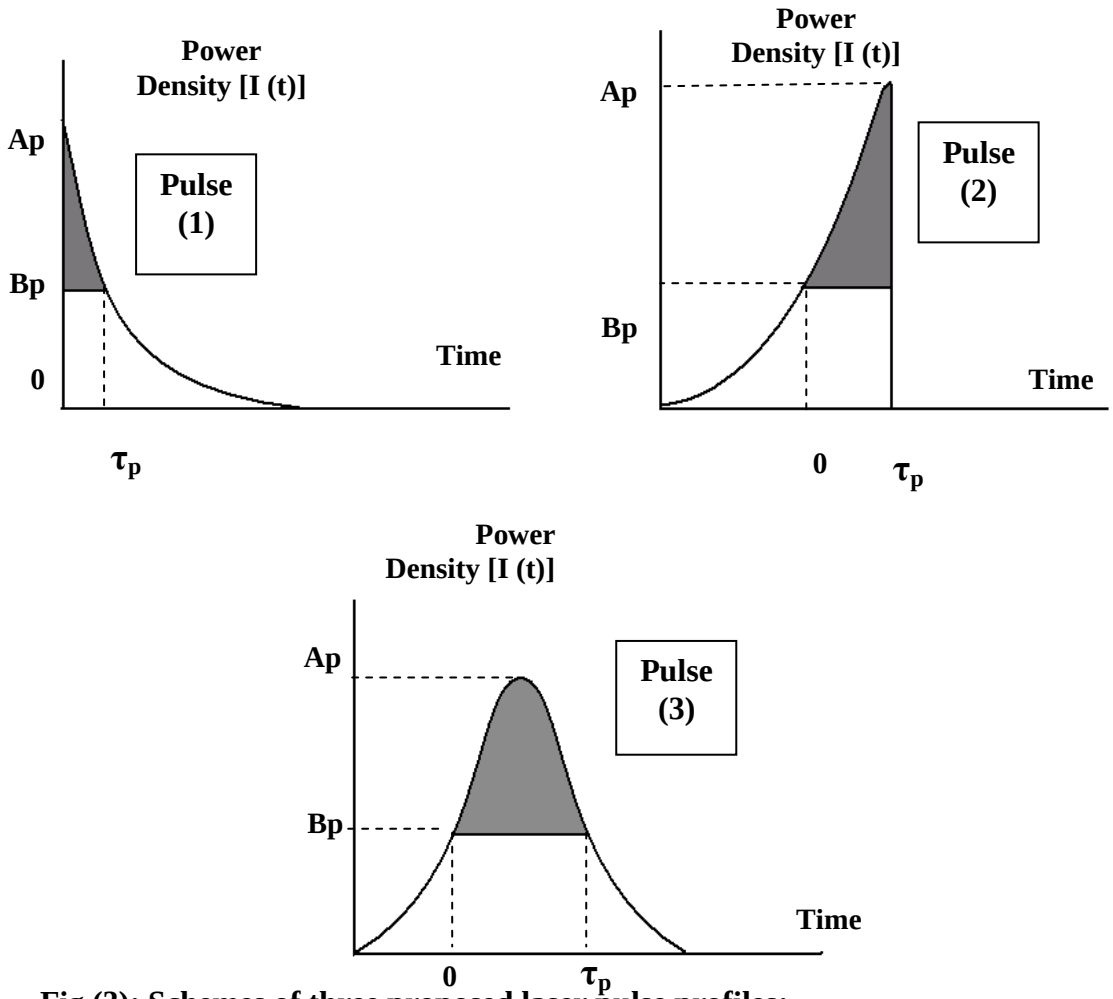

Fig (3): Schemes of three proposed laser pulse profiles:
Pulse (1): Exponentially decreasing.
Pulse (2): Exponentially increasing.
Pulse (3): Gaussian shape.
***- The shaded portions of the profiles are formulated in mathematical representations of the present model.**

***- Values of Ap and Bp are chosen so that the average power density** $(\int_0^{\tau_p} I(t)dt/\tau_p)$ **lies within the range of LSAW- formation.**

Properties of the three pulse types are summarized in the following table:

Table (1): Mathematical features of laser pulses employed in the calculations of this work.

***:** $\bar{I}$ **is determined here for A_p=2x10^6 W/cm^2, B_p=10^6 W/cm^2 and τ_p=20 μs.**

Pulse	Mathematical form of power density { I(t) }	μ – factor	Average Power Density $(\bar{I})^*$:
Pulse (1) Exponentially Decreasing	$I=A_p e^{-\mu t}$	$\mu=\ln(A_p/B_p)/\tau_p$	$\bar{I}=(A_p/\mu\tau_p)(1-e^{-\mu\tau_p})$ =1.4x10^6 W/cm^2
Pulse (2) Exponentially Increasing	$I=B_p e^{\mu t}$	The same μ of Pulse (1)	$\bar{I}=(B_p/\mu\tau_p)(e^{\mu\tau_p}-1)$ = 1.4x10^6 W/cm^2
Pulse (3) Gaussian	$I=A_p e^{-\mu(t_O-t)^2}$ $t_o=\tau_p/2$	$\mu=4\ln(A_p/B_p)/\tau_p^2$	$\bar{I}$ =1.6x10^6 W/cm^2 { found by numerical integration of I(t) }

It may be noticed from table (1) that values of A_p and B_p were chosen so that average power density values lie within the range of LSAW- formation.
Other forms of laser pulses were proposed such as [7]:

$$\phi_{las} = \frac{4E}{\pi\tau d^2}\exp[-(\frac{t-12\tau}{\tau})^2] \ldots (4)$$

where (Φ_{las}) is the laser pulse flux density and (d) represents the laser spot diameter on target surface. In this form, the pulse duration is represented via a characteristic time scale (τ) and a characteristic energy (E) [7]. Obviously, the term multiplied by the exponential is a power density factor (power per unit area) and the exponential represents temporal Gaussian distribution. Another proposed expression for laser pulse given as [8]:

$$I_s(r,t) = I_o h(t) e^{-r^2/\omega^2} \quad \ldots. (5)$$

where (I_o) is the average power density, and (r) is the laser spot-radial axis on target surface of centre at r=0. In this expression it is assumed that laser irradiation is restricted over a fixed circular spot of radius (ω) [8].
The exponential factor in eq. (5) is a Gaussian spatial distribution of power density, while temporal evolution is described by the factor h(t) via suitable functions of time, provided $|h| < 1$ [8].

Present Model Calculations

The main aim of the present calculations is to solve eq.(3) numerically for different mathematical forms of laser power pulse density (I).
In order to monitor the surface temperature evolution throughout a single laser pulse, the whole range of ξ (i.e. ξ=0 to 1) is divided into subintervals and the integration of eq.(3) is performed numerically for each subinterval starting from a lower limit (which represents the fixed lower limit for all subintervals) to the upper limit of the subinterval. This process is repeated for all subintervals in a successive manner until reaching the end of the pulse at ξ=1.
It should be mentioned that it was not possible to start the numerical integration from a zero lower limit because of the $\{(\xi')^{1/2}\}$ factor in the denominator of the integrand of eq.(3). The lower limit of this integration is approximated as $(\Delta\xi')$ which is the time step of the numerical procedure employed. This is illustrated schematically in fig.(4).
By investigation of that integrand, two types of quantities may be classified, they may be referred to as time ascending- and time descending-development quantities.
For a given upper limit (ξ) of a subinterval, it is noticed that quantities like power density $I(\xi-\xi')$ and the time factor $(\xi-\xi')$ in the denominator {multiplied by the blast velocity (V_B)} are of a descending time nature, where the argument $(\xi-\xi')$ decreases with the development of (ξ'). On the other hand, the quantity $\{(\xi')^{1/2}\}$ in the denominator is of an ascending time nature. These two types of time dependent quantities should be treated before performing the numerical integration for each subinterval. For any subinterval, the normalized time (ξ') proceeds by a time step $(\Delta\xi')$ in the numerical calculations.Numerical integration of eq.(3) is performed by generating two sets of data throughout the time progression in each subinterval. Set (A) which involves values of both $[I(\xi')]$ and $[\xi']$ among a given subinterval, they are separated by step $(\Delta\xi')$. Similarly, set (B) is generated; it involves the quantity $[(\xi')^{1/2}]$ among that subinterval. For all of those quantities generated in sets [A] and [B] , the normalized time factor (ξ') is of an

increasing nature. For any subinterval, the integration normalized time (ξ') begins at the beginning point of a subinterval ($\Delta\xi'$) {which is a common starting point for all subintervals} and ends at the upper limit of that subinterval {the lower and upper limits of the integration in eq.(3)}. To start the numerical integration, data in one of those sets [say set (B)] is reversed in order. Hence two data sets are obtained, one of a descending- and the other of an ascending- time development nature. Now the integration may be performed numerically (trapezoidal rule is employed) throughout a subinterval to determine surface temperature at the end of that subinterval. The upper limit of the integration is then increased and the previous procedure is performed for the next (longer) subinterval starting from the same lower limit of integration ($\Delta\xi'$). This is illustrated in fig.(5) for a given subinterval.

The above process is repeated for the successively increasing subintervals to obtain the temperature at the end of each subinterval until reaching the end of the laser pulse at the upper limit ξ=1.

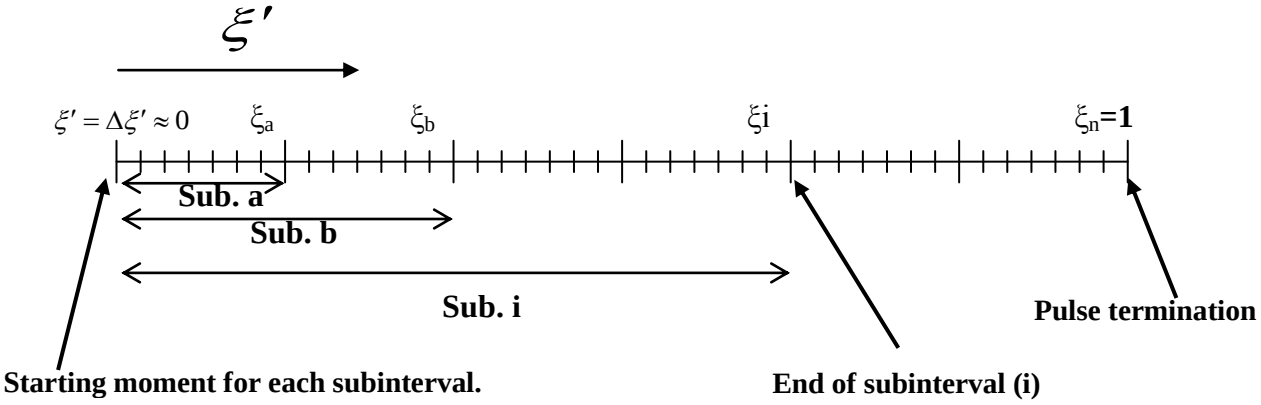

Fig.(4) Division of pulse duration into subintervals:

*- Each subinterval is divided by time step ($\Delta\xi'$).

*- All subintervals start at the same moment ($\xi' = \Delta\xi' \approx 0$) which represents the lower limit of the integral in eq.(3).

*- Successive subintervals (Sub. a, Sub. b, …) end at successively increasing ending moments ($\xi_a<\xi_b<\ldots$) each represents the upper limit (ξ) of the integration in eq.(3).

*- Solving eq.(3) for successive subintervals yields surface temperature at moments ξ_a, ξ_b, …, ξ_n throughout laser pulse duration.

Set [A]		Set [B] Before Reversal	Set [B] After Reversal
ξ_1	$I(\xi_1)$	$\xi_1^{1/2}$	$\xi_a^{1/2}$
ξ_2	$I(\xi_2)$	$\xi_2^{1/2}$	$\xi_{a-1}^{1/2}$
ξ_3	$I(\xi_3)$	$\xi_3^{1/2}$	$\xi_{a-2}^{1/2}$
.	.	.	.
.	.	.	.
.	.	.	.
ξ_{a-2}	$I(\xi_{a-2})$	$\xi_{a-2}^{1/2}$	$\xi_3^{1/2}$
ξ_{a-1}	$I(\xi_{a-1})$	$\xi_{a-1}^{1/2}$	$\xi_2^{1/2}$
ξ_a	$I(\xi_a)$	$\xi_a^{1/2}$	$\xi_1^{1/2}$

Fig (5): An illustration of preparing data to integrate eq.(3) numerically for a given subinterval {Sub. a in fig.(4)}.

*- Quantities involved in numerical integration are those in set [A] and set [B]\ after reversal with order as indicated for these two sets.

*- This procedure is performed for all successively increased subintervals till the termination point of the laser pulse.

Results and Discussion:

In reference [6], eq.(1) was integrated analytically to obtain target surface temperature evolution through the action of an incident laser pulse of a constant magnitude (Pc) {i.e. square pulse (see fig.(2)}. The related parameters were as follows [6]:
$Pc=1x10^6$ W/cm^2, τp=20μs, ro=0.1cm, V_B=500m/s, and μeff=0.2. Thick aluminum target was considered with initial temperature of zero ºC. The result of that determination is shown in fig.(6). The trend of the curve in this figure was explained in Ref.[6].

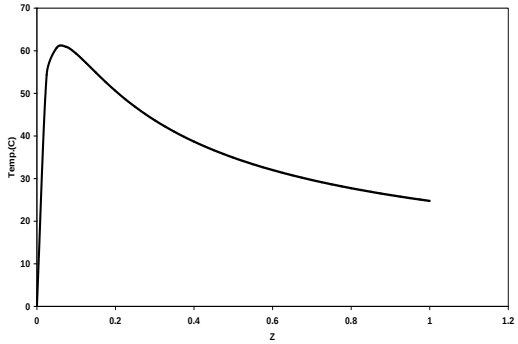

Fig.(6): Surface temperature vs. normalized time (z) {orξ}. Laser Pulse:Square pulse ($Pc=1x10^6$W/cm^2) r_o=0.1cm, τ_p=20μs, μ_{eff} =0.2.

For the present model, the three proposed pulses {Illustrated in fig.(3) and table (1)} are examined. Figures (7)-(9) represent comparisons between results of the present model and the analytic results of the square pulse [6], all determined under the same related parameters mentioned above.
For comparison purpose, the constant amplitude of the square pulse {Pc in Fig.(2)} is taken equal to the average value ($\bar{I}$) of the corresponding proposed pulse with which it is being compared {see average power density of proposed pulses in table (1)}. It is noted from figs.(7)-(9) that the curves of the present model and the analytic curves of the square pulses have the same trend; the differences in calculated temperatures in each of those figures are largely referred to the rule of pulse shape (profile) in determining surface temperature evolution in time.
Figure (7) indicates that exponentially increasing pulse {pulse (2) in fig.(3)} yields less heating effect compared with the square pulse. This may be explained by noting the shapes of the square pulse and pulse (2) {figs.(2) and (3)}, where the power density is at a steady level all over the square pulse duration [this steady level is equal to the average power density of the conjugate pulse {pulse (2)}]. On the other hand, the power density of the exponentially increasing pulse is well below its average level for the major part of pulse duration; however, it exceeds the average level only during a minor part of the pulse period after which the pulse is terminated with no more power support.
A similar situation is observed in fig.(8) where the proposed Gaussian pulse {pulse (3) in fig.(3)} is compared with a square pulse. As in fig.(7), the magnitude of the square pulse is equal to the average power density of the Gaussian pulse with which it is being compared. Here too, the square pulse yields higher temperatures compared with the Gaussian pulse. Explanation of fig.(8) is similar to that of fig.(7), where the Gaussian power density exceeds the average level around the centre of the pulse period (τ_p/2) while the major part of the pulse is below the average level. On the other hand, the square pulse maintains this level for the whole duration (τ_p).

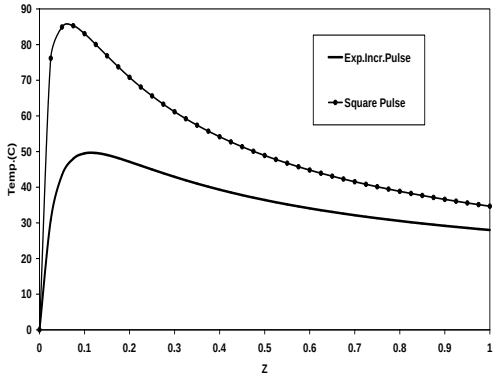

Fig.(7): Surface temperature vs. normalized time. A comparison between square- and exponentially increasing- pulses. Pc=$(\bar{I})$ = 1.4x10^6 W/cm^2.

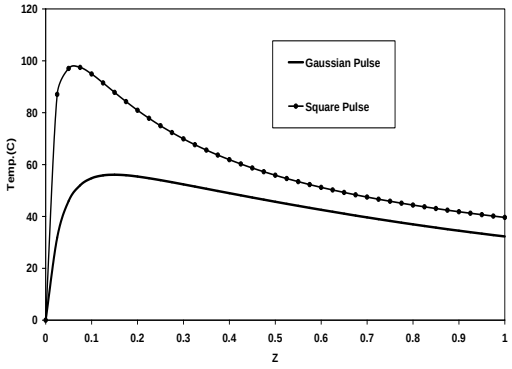

Fig.(8): Surface temperature vs. normalized time. A comparison between square- and Gaussian-pulses. Pc= $(\bar{I})$ = 1.6x10^6 W/cm^2.

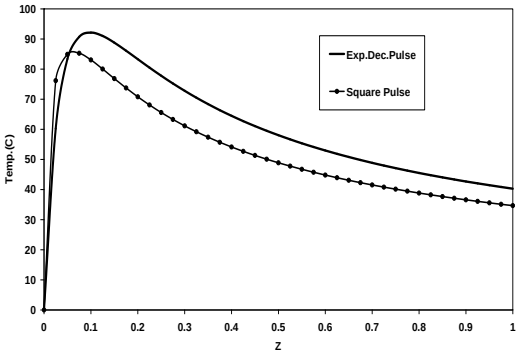

Fig.(9): Surface temperature vs. normalized time. A comparison between square- and exponentially decreasing- pulses. Pc=$(\bar{I})$ = 1.4x10^6 W/cm^2.

In fig.(9) a comparison is illustrated between the proposed exponentially decreasing pulse {pulse (1) in fig.(3)} and the corresponding square pulse. It is noted that pulse (1) results the higher temperatures. By examining pulse (1) in fig.(3) and table (1), one may recognize that the power density exceeds the average level at the beginning of the pulse, and then it decays exponentially when time proceeds. However, the exponential decay tail of the pulse acts to support the high scale heating caused by the initially- high power densities of the pulse. In other words, the exponential tail sustains surface temperature through subsequent incident power deposition on the surface. This will slows down the rate of temperature decrease with time during pulse duration.

The conclusion that may be extracted from figs.(7)-(9) is that the time distribution of power in a laser pulse (i.e. the pulse shape) plays a rule in determining the temperature evolution at the target surface. It is believed that constant average power by itself is insufficient for this purpose; moreover, the square pulse is an ideal representation of real laser pulses. Different pulse profiles lead to different temperature evolution history at target surface as illustrated in fig.(10) which shows the time variation of surface temperature for the three proposed pulse expressions shown in fig.(3) and given in table (1).

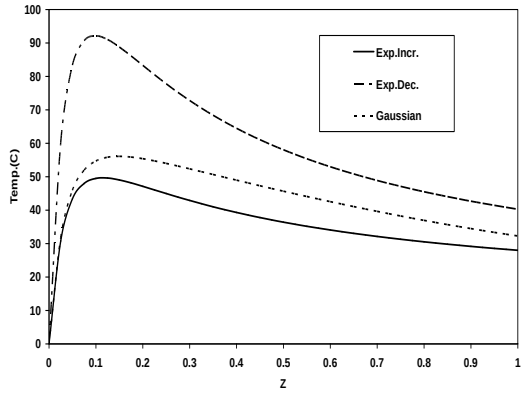

Fig.(10): Surface temperature vs. normalized time. A comparison for the three proposed laser pulses.

Considering other laser pulses, the profile given in eq. (4) seems to have some scaling or characteristic factors, hence it is expected that those factors have to be chosen carefully in order to represent a given laser pulse mathematically. This will add further complexity in formulating laser pulses properly.

On the other hand, it is believed that the spatial distribution (e^{-r^2/ω^2}) in the profile given by eq.(5), {not appearing in the three profiles in Table (1)} is not required when dealing with LSA plasma since this plasma acts to distribute laser energy (in the form of heat) uniformly among target affected area (plasma – target interface).

Moreover the fixed radius (ω) for laser irradiation over targets surface indicates that expression (5) does not take into account plasma expansion, which is the case under study in this work.

Finally, a comparison may be achieved between square pulse- and time varying pulse- approaches, which is based on the final temperature concept. The final temperature of target surface (determined at ξ=1) accounts for the net amount of heat energy on target surface at the end of a single laser pulse despite the temporal details of temperature evolution during the pulse duration {in which the two models differ}. In other words, final surface temperature accounts for the overall heating effect on the surface during the whole pulse duration, where eq.(3) takes into account both heat energy gain on the surface due to incoming power from incident laser pulse, and heat energy loss at the surface due to heat flow toward the target bulk via heat conduction. The final temperature may be correlated with the average (constant) power density since this average is correlated to the overall heating effect of the incident power density throughout the whole pulse duration. Since the steady power density (Pc) of the square pulse and the average power density $(\bar{I})$ of the time varying pulse are taken to be equal in each of the comparison figures {figs.(7)-(9)}, then it is expected that final temperatures resulted by the two types of pulses to approach each other at the end of the duration as may be noticed in figs.(7)-(9). In figs.(7) and (8), large deflection in instantaneous temperature may be observed for the two pulses under comparison during the first half of the pulse (which reflects the differences in instantaneous power densities).However, the temperature curves get closer to each other continuously during the second half of the pulse till the end of the duration at ξ=1.

References:

1. Annemie Bogaerts, Zhaoyang Chen, Renaat Gijbels, Akos Vertes. 2003. Laser ablation for analytical sampling: what can we learn from modeling?. Spectrochimica Acta Part B 58: 1867-1893.
2. Gupta G. P., Suri B. M. 2004. Vapor and plasma ignition thresholds for visible pulsed- laser ablation of metallic targets, Applied Surface Science (A.S.S.) 230: 398- 403.

3. Annemie Bogaerts, Zhaoyang Chen. 2005. Effect of laser parameters on laser ablation and laser induced plasma formation : A numerical modeling investigation, Spectrochimica Acta Part B 60: 1280-1307.
4. Sturmer, E. and von Allmen, M. 1978. Influence of laser supported detonation waves on metal drilling with pulsed CO_2 lasers, J. Appl. Phys 49(11):5648-5654.
5. Pirri, A.N., Root, R.G., and Wu, P.K.S. 1978. Plasma Energy Transfer to Metal surfaces Irradiated by Pulsed Lasers, AIAA Journal 16(12): 1296-1304.
6. Robin, James E. 1978. Pulsed laser heating of thick opaque targets in air, J. Appl. Phys., 49 (10): 5306-5310.
7. Morel, V., Bultel, A., Benredjem, D., Cheron, B. G. 2009. Laser creation of aluminum plasma from a solid target: A model, 29th ICPIG, July 12-17, Cancun, Mexico, Topic No.:6.
8. Shannon, Mark A., Rostami, Ali A., and Russo, Richard E. 1992. Photo thermal deflection measurements for monitoring heat transfer during modulated laser heating of solids, J. Appl. Phys. 71 (1): 53-63.

التسخين الليزري احادي النبضة للأجسام المعتمة في الهواء

بسام حنا حبيب*

*كلية المنصور الجامعة / هندسة اتصالات الحاسبات

الخلاصة:

تم تطوير نموذج نظري لأحتساب التغير الزمني لدرجة الحرارة لسطح مادة صلبة معتمة موضوعة في الهواء الجوي خلال تعرضها لنبضة ليزرية و لحالات محددة تسمح بتولد البلازما على هيئة ما يعرف بموجات الأمتصاص المعززة بالليزر [Laser supported Absorption Waves (LSAW)] . يتم في النموذج الحالي التعامل مع التغيرات الزمنية لشدة النبضة, أو كما يعرف بشكل النبضة, من حيث تأثيرها على نمط التغيرات الزمنية لدرجة الحرارة عند سطح الهدف. تم اقتراح ثلاثة اشكال للنبضة الليزرية و جرت مقارنة تأثيراتها الحرارية مع حالة النبضة المربعة ذات الشدة الثابتة.